Fatigue-Crack Propagation in Gamma-Based Titanium Aluminide Alloys at Large and Small Crack Sizes

J. J. Kruzic, J. P. Campbell and R. O. Ritchie
Materials Sciences Division, Lawrence Berkeley National Laboratory, and Department of Materials Science and Mineral Engineering, University of California, Berkeley, CA 94720-1760

ABSTRACT

Most evaluations of the fracture and fatigue-crack propagation properties of $\gamma + \alpha_2$ titanium aluminide alloys to date have been performed using standard "large-crack" samples, e.g., compact-tension specimens containing crack sizes which are on the order of tens of millimeters, i.e., large compared to microstructural dimensions. However, these alloys have been targeted for applications, such as blades in gas-turbine engines, where relevant crack sizes are much smaller (<500 μm) and where the small-crack fatigue threshold may be the most relevant design parameter. In this study, we compare and contrast the cyclic crack-growth behavior of both large (a > 5 mm) and small (c ~ 25–300 μm) cracks in a γ-TiAl based alloy, of composition Ti-47Al-2Nb-2Cr-0.2B (at.%), specifically for duplex (average grain size ~17 μm) and refined lamellar (average colony size ~150 μm) microstructures. It is found that, whereas the lamellar microstructure displays far superior fracture toughness and fatigue-crack growth resistance in the presence of large cracks, in small-crack testing the duplex microstructure exhibits a better combination of properties. The reasons for such contrasting behavior are examined in terms of the intrinsic and extrinsic (i.e., crack bridging) contributions to cyclic crack advance.

INTRODUCTION

Two-phase gamma-TiAl based intermetallic alloys have received considerable attention in recent years as candidate materials for high-temperature aerospace and automotive applications, in particular as possible replacements for conventional nickel and titanium alloys in gas turbines [1-4]. Two conditions have been prominent: a duplex microstructure, consisting of equiaxed grains of γ (TiAl) with small amounts of α_2 (Ti_3Al) grains, and a lamellar microstructure, consisting of lamellar colonies containing alternating γ and α_2 platelets. In general, duplex structures display better elongation and strength properties, whereas lamellar structures show better creep resistance, toughness, and (large-crack) fatigue-crack growth resistance [1,2,5-8].

Although duplex structures have somewhat higher 'smooth-bar' fatigue limits [4,9], fatigue-crack growth properties, conventionally measured using *large-crack* specimens containing >5 mm long cracks, are clearly superior in lamellar structures [4,8,10-13]. However, preliminary indications are that this benefit is lost when tests are performed on small (<500 μm) surface cracks [13]. As many potential applications for γ-TiAl alloys may involve fatigue design based on a small-crack threshold, the current work is focused on a comparison of large- and small-crack growth behavior in γ-TiAl based alloys and on the specific role of microstructure in influencing such behavior.

EXPERIMENTAL PROCEDURES

Duplex and lamellar microstructures (~10 vol.% α_2) were studied in a γ-based alloy of composition Ti-47Al-2Nb-2Cr-0.2B (at.%); the B additions resulted in ~0.5 vol.% of needle-like TiB_2 particles (~ 2-10 μm in length, ~1 μm in diameter). The lamellar microstructure (Fig. 1a) was obtained by forging and subsequent heat treating at 1370°C in flowing argon for 1 hr, air cooling and then holding

Mat. Res. Soc. Symp. Proc. Vol. 552 © 1999 Materials Research Society

for 6 hr at 900°C prior to argon furnace cooling. The resulting microstructure consisted of ~145 μm-sized lamellar colonies (α_2 center-to center spacing of ~1.3 μm) with very small amounts (~4%) of fine equiaxed γ grains (5-20 μm) between lamellar colonies. The corresponding duplex microstructure (Fig. 1b) was achieved by forging and subsequent heat treating at 1320°C in argon for 3 h, followed by argon furnace cooling. This microstructure consisted of nearly equiaxed grains of the γ-phase, ~17 μm in diameter, with the α_2 phase appearing along γ grain boundaries and at triple points.

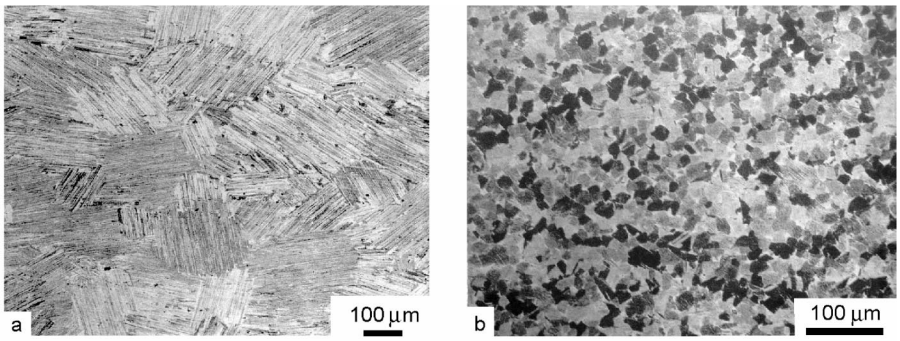

Figure 1. Optical micrographs of the (a) lamellar and (b) duplex microstructures of a Ti-47Al-2Nb-2Cr-0.2B (at.%) alloy. (Etched with 2% HF, 5% H_3PO_4 etchant)

The growth of small surface cracks (c ~ 25-300 μm) was evaluated in room temperature air using unnotched, 6-mm thick, rectangular beams loaded in four-point bending. Samples were cycled at a positive load ratio (ratio of minimum to maximum load) of R = 0.1 at frequencies between 5 and 25 Hz (sine wave). Small surface cracks were initiated from electro-discharge machining (EDM) pit damage generated on the tensile-loaded beam surface for both microstructures and in the case of the lamellar microstructure cracks were also naturally initiated by cycling polished samples. Data from both techniques were comparable. EDM pitted samples were cyclically loaded to grow the cracks away from the heat-affected zone (HAZ) prior to data acquisition; some sample surfaces were ground and polished following pitting to eliminate the EDM damage, leaving only small surface cracks that originated from the pitting process.

Fatigue-crack growth was observed by periodically interrupting the test, at which time cracks were either observed directly on the sample surface or on metal-coated surface replicas using optical microscopy. Replication was performed with the sample under load using cellulose acetate tape softened with acetone. Growth rates were computed from the amount of crack extension between two discrete measurements; specifically, each data point represents the average growth rate and ΔK value, with the error bars representing the range of ΔK within the increment. Stress intensities were determined using linear-elastic solutions for surface cracks in bending [14]. Based on heat-tinting studies on several samples, a semi-circular crack profile (crack depth to half-surface crack length ratio of a/c = 1) was considered.

RESULTS

Fatigue-Crack Propagation of Large Cracks

It is well documented that lamellar microstructures in γ-TiAl based intermetallics possess superior fatigue-crack growth resistance to that of duplex microstructures, *but only in the presence of large* (>5 mm) *cracks* [4,8,10]. Such superior performance of lamellar structures is evident in Fig. 2 which shows the relative crack-growth rates of large (through-thickness) cracks in several duplex and lamellar alloys, including those studied herein [11,12]. It is clear that the lamellar alloys have the higher threshold (ΔK_{TH}) values and lower Paris power-law exponents.

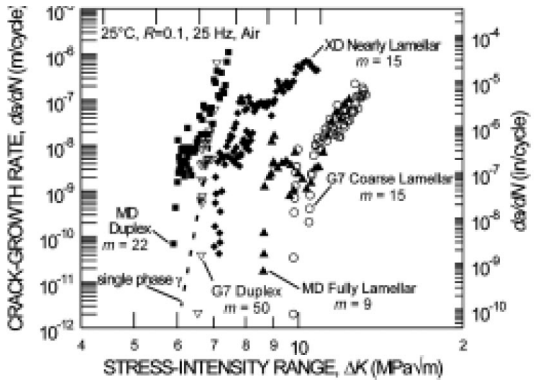

Figure 2. A comparison of the fatigue-crack growth resistance of a fine nearly-lamellar microstructure Ti-47.7Al-2.0Nb-0.8Mn (XD) alloy, both duplex and fine fully-lamellar microstructure Ti-47Al-2Nb-2Cr-0.2B (MD) alloy, both duplex and coarse lamellar microstructures in a Ti-47.5Al-2.3Nb-1.5Cr-0.4V (G7) alloy and a single phase γ alloy (Ti-55Al with traces of Nb, Ta, C, and O) [11,12].

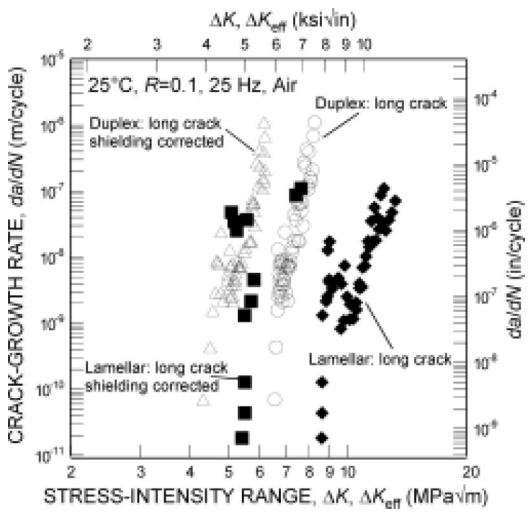

Figure 3. Comparison of the large-crack (a > 5 mm) fatigue-crack growth results, plotted as a function of the applied stress-intensity range, ΔK, and in terms of the "shielding-corrected" stress-intensity range, ΔK_{eff} for the duplex and lamellar microstructures [11,12].

Crack-growth rates specifically for large, through-thickness cracks in the present duplex and lamellar microstructures are shown in Fig. 3. When results are compared in terms of the applied stress-intensity range, ΔK, growth rates in the lamellar structure are up to five orders of magnitude lower, and threshold, ΔK_{TH}, values are some 50% higher, than in the duplex structure. This behavior has been attributed primarily to enhanced crack-tip shielding in the lamellar structure, primarily from crack bridging due to uncracked (shear) ligaments, generated by inter-and intra-lamellar cracking *ahead* of the tip [5-13]. Consequently, behavior in the two microstructures becomes similar when growth rates are characterized *intrinsically* in terms of the effective (shielding-corrected) ΔK_{eff}, defined as $\Delta K_{eff} = (K_{max} - K_{br}) - K_{cl}$, where K_{br} is the reduction in K_{max} due to bridging and K_{cl} is the crack closure stress intensity when the crack faces first come into contact [11,12]. Methods of measurement of these values are described elsewhere [11,15].

Large- vs. Small-Crack Growth

A comparison of the growth-rate behavior of small (c ~ 25–300 μm) surface cracks and large (a > 5 mm) through-thickness cracks in the duplex and lamellar structures, are shown in Figs. 4a and

4b, respectively; the large-crack data are shown both before and after accounting for shielding. From these results and others [13,16-19], it is apparent that:

- At the same applied ΔK levels, the growth rates of the small cracks in both microstructures exceed those of corresponding large cracks by up to several orders of magnitude.
- Small-crack growth is seen at applied stress intensities below the large-crack ΔK_{TH} thresholds.

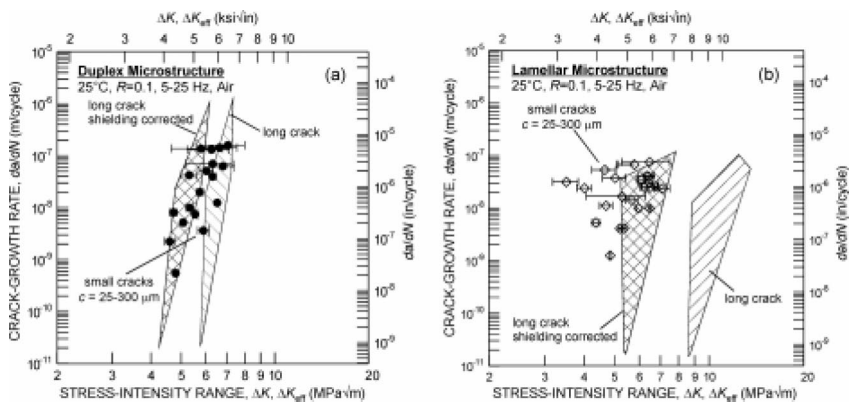

Figure 4. Comparison of small- (c ~ 25-300 μm) and large-crack growth rates during the fatigue of a) duplex and b) lamellar microstructures, where the large-crack data (from Fig. 3) are plotted in terms of both the applied ΔK and near-tip "shielding-corrected" ΔK_{eff}. Error bars represent the range of ΔK values over specific growth increments.

- Although superior large-crack fatigue properties are seen for the lamellar microstructure, the growth rates for small cracks in the duplex and lamellar microstructures are comparable.
- Despite the similarity of small-crack growth rates in the two microstructures, there is significantly more scatter in the coarser lamellar microstructure. Furthermore, small cracks in this microstructure are able to grow, at significant growth rates ($da/dN \sim 5 \times 10^{-8}$ m/cycle), at applied ΔK levels well below those for equivalent crack growth in the duplex structure.

Origin of the Small-Crack Effect: Limited Crack-Tip Shielding

Comparison of small-crack growth rates with the *intrinsic* large-crack rates, i.e., where the crack-tip shielding has been accounted for in terms of ΔK_{eff}, results in a much closer correlation between the data sets than that provided by comparison with the measured (non-shielding-corrected) large-crack data. This suggests that the small-crack growth rates are faster than those of corresponding large cracks because of their limited wake, which limits the development of equilibrium shielding zones behind the tip. In essence, this implies that the small-crack growth rates reflect the intrinsic crack-growth resistance, akin to the "shielding-corrected" large-crack behavior; however, this is only true where crack sizes are small compared to the shielding-zone lengths (similitude limitation) yet still large compared to microstructural dimensions.

For the duplex microstructure, the shielding-corrected large-crack growth-rate data provide a useful reference curve for design against fatigue in the presence of small flaws. Examination of Fig. 4a indicates that the small cracks do not grow below the "shielding-corrected" large-crack threshold, $\Delta K_{eff,TH}$. It is thus possible to define a lower-bound threshold in this microstructure below which neither large nor small cracks (c > 25 μm) will propagate, using crack-growth rate data acquired from standard "large-crack" samples, plotted as a function of ΔK_{eff}.

In contrast, in the lamellar microstructure, small cracks are observed to grow at applied stress intensities *below* the large-crack $\Delta K_{eff,TH}$. Indeed, the absence of a definable, lower-bound threshold below which small cracks will not propagate in lamellar γ-based TiAl alloys has been reported previously [13,16-19]. These results suggest that a limited equilibrium shielding zone, although a major factor, is not the only cause of the small-crack effect in lamellar structures.

Origin of the Small-Crack Effect: Biased Microstructural Sampling

In addition to being small compared to shielding-zone lengths, cracks in the lamellar structure can also be regarded as small with respect to microstructural dimensions (continuum limitation) since the average colony size (~145 μm) is on the same order of magnitude as the cracks under study (c ~ 25–300 μm). The influence of the coarser lamellar structure on small-crack behavior is apparent in Fig. 5, where the small-crack data are further divided into cracks with initial surface crack lengths smaller and larger then the average colony size. From this comparison, it is apparent that all the small cracks that were observed to propagate below the "shielding-corrected" large-crack threshold had initial crack lengths smaller than the average colony size, while no small cracks with initial crack lengths larger then the average colony size grew at $\Delta K < \Delta K_{eff,TH}$. Although using the average colony size as the critical microstructural dimension is somewhat arbitrary, it does demonstrate that, for cracks contained within one or two lamellar colonies, the growth behavior is different from that observed when the crack front samples many colonies.

This result is not surprising considering observations [20] of the strong preference for crack initiation parallel to the lamellar interface orientation, and the tendency for cracks to arrest at colony boundaries. These observations are further supported by numerous studies that have found large cracks to grow at different rates at the same applied ΔK levels depending on the crack orientation relative to the lamellar interfaces [21-23].

CONCLUSIONS

Based on a study of small fatigue-crack growth in duplex and lamellar microstructures in a γ-based Ti-47Al-2Nb-2Cr-0.2B (at.%) alloy, the following conclusions can be made:

- Growth rates of small (c < 300 μm) cracks in both microstructures were found to exceed that of large cracks for a given applied (far-field) stress-intensity range.
- Additionally, small cracks grew at applied ΔK levels below the large-crack fatigue threshold.
- Such small-crack effects were rationalized in terms of limited crack-tip shielding and in the case of the lamellar microstructure, biased microstructural sampling.

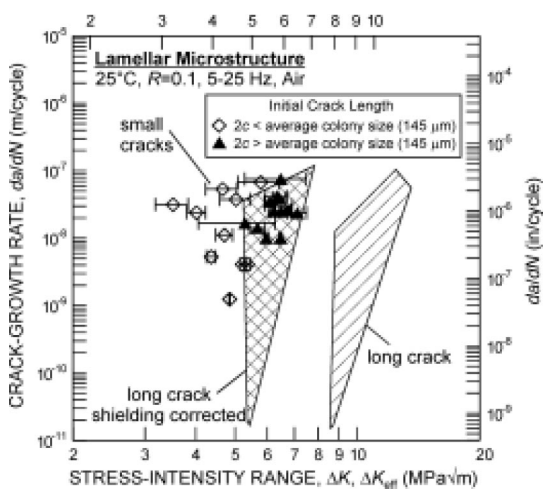

Figure 5. Fatigue-crack growth-rate behavior for small cracks in the lamellar microstructure compared to large-crack data as a function of ΔK and ΔK_{eff}. Note that the small-crack growth rates are only consistent with the shielding-corrected large-crack data where surface crack sizes are larger than the average colony size ($2c$ > 145 μm). Error bars represent the range of ΔK values over specific crack-growth measurement increments.

- Although the lamellar microstructure displays far better *large-crack* fatigue-crack growth resistance, for applications such as gas-turbine blades where fatigue design must be based on the notion of *no* crack growth, the duplex microstructure appears to offer the more attractive properties, namely a definable lower-bound small-crack threshold that can be obtained from "shielding-corrected," large-crack results.

ACKNOWLEDGMENTS

This work was supported by the Office of Energy Research, Office of Basic Energy Sciences, Materials Sciences Division of the U.S. Department of Energy under Contract No. DE-AC03-76SF00098. Large-crack data were from earlier programs supported by the Air Force Office of Scientific Research. The authors thank Dr. D. S. Shih (McDonnell-Douglas) for supplying the alloy, and Dr. K. T. Venkateswara Rao (Guidant Corp.) for numerous helpful discussions.

REFERENCES

1. Y-W. Kim and D. M. Dimiduk, JOM 43(8), 40-47 (1991).
2. Y-W. Kim, JOM 46(7), 30-40 (1994).
3. G. F. Harrison and M. R. Winstone, in Mechanical Behavior of Materials at High Temperature, edited by C. Moura Branco, R. O. Ritchie and V. Sklenicka (Kluwer Academic Publishers: NATO ASI Series, 1996), pp. 309-325.
4. J. M. Larsen, B. D. Worth, S. J. Balsone and J. W. Jones, in Gamma Titanium Aluminides, edited by Y-W. Kim, R. Wagner and M. Yamaguchi (TMS, Warrendale, PA, 1995), pp. 821-834.
5. K. S. Chan and Y-W. Kim, Metall. Trans. 23A, 1663-1677 (1992).
6. K. S. Chan, Metall. Trans. 24A, 569-583 (1993).
7. K. S. Chan and Y-W. Kim, Metall. Trans. 24A, 113-125 (1993).
8. K. T. Venkateswara Rao, Y-W. Kim, C. L. Muhlstein and R. O. Ritchie, Mater. Sci. Eng. A192, 474-482 (1995).
9. J. Kumpfert, Y-W. Kim and D. M. Dimiduk, Mater. Sci. Eng. A192/193, 465-473 (1995).
10. S. J. Balsone, J. M. Larsen, D. C. Maxwell and J. W. Jones, Mater. Sci. Eng. A192/193, 457-464 (1995).
11. J. P. Campbell, K. T. Venkateswara Rao and R. O. Ritchie, Mater. Sci. Eng. A239-240, 722-728 (1997).
12. J. P. Campbell, K. T. Venkateswara Rao and R. O. Ritchie, Metall. Mater. Trans. 30A(2) in press (1999).
13. J. P. Campbell, A. L. McKelvey, S. Lillibridge, K. T. Venkateswara Rao and R. O. Ritchie, in Deformation and Fracture of Ordered Intermetallic Materials IV: Titanium Aluminides, edited by W. O. Soboyejo, T. S. Srivatsan and H. L. Fraser (TMS, Warrendale, PA, 1996), pp. 141-157.
14. J. C. Newman and I. S. Raju, Eng. Fract. Mech. 15, 185-192 (1981).
15. R. O. Ritchie and W. Yu, in Small Fatigue Cracks, edited by R. O. Ritchie and J. Lankford (TMS-AIME, Warrendale, PA, 1986), pp. 167-189.
16. J. P. Campbell, J. J. Kruzic, S. Lillibridge, K. T. Venkateswara Rao and R. O. Ritchie, Scripta Mater. 37, 707-712 (1997).
17. K. S. Chan and D. S. Shih, Metall. Mater. Trans. 28A, 79-90 (1997).
18. K. S. Chan and D. L. Davidson, in Structural Intermatallics, edited by R. Darolia, J. J. Lewandowski, C. T. Liu, P. L. Martin, D. B. Miracle and M. V. Nathal (TMS, Warrendale, PA, 1993), pp. 223-230.
19. K. S. Chan and D. S. Shih, Metall. Mater. Trans. 29A, 73-87 (1998).
20. J. J. Kruzic, J. P. Campbell and R. O. Ritchie, Acta Mater. 47, in press (1999).
21. R. Gnanamoorthy, Y. Mutoh, K. Hayashi and Y. Mizuhara, Scripta Metall. Mater. 33 (6), 907-912 (1995).
22. D. L. Davidson and J. B. Campbell, Metall. Trans. 24A 1555-1574 (1993).
23. P. Bowen, R. A. Chave and A. W. James, Mater. Sci. Eng. A192/193 443-456 (1995).